ELSEVIER

Contents lists available at ScienceDirect

Biomaterials Advances

journal homepage: www.journals.elsevier.com/materials-science-and-engineering-c



Enhanced anti-*P. aeruginosa* treatment via phage and ciprofloxacin co-loaded particles prepared by electrospraying

Sai Liu^a, Andrew Weston^a, Giovanni Satta^b, Sara Bolognini^c, Mariagrazia Di Luca^c, Simon Gaisford^a, Gareth R. Williams^{a,*}

- ^a UCL School of Pharmacy, University College London, 29-39 Brunswick Square, London, WC1N 1AX, UK
- ^b Centre for Clinical Microbiology, University College London, Royal Free Campus, Rowland Hill Street, London, NW3 2PF, UK
- ^c Department of Biology, University of Pisa, Via San Zeno, 39 56127, Pisa, Italy

ARTICLE INFO

Keywords: Electrospraying Anti-microbial resistance Drug delivery Phages Ciprofloxacin

ABSTRACT

Antimicrobial resistance (AMR) poses a critical global health challenge, contributing to an estimated 1.27 million deaths worldwide due to bacterial infections in 2019. Phages offer a possible solution to this, but alone have been found to be sub-optimal. There can however be great benefits in combining antibiotics and phages to give synergistic treatment. To that end, this study incorporates both ciprofloxacin (cipro) and phages into co-loaded microparticles prepared by electrospraying (ES). With optimized concentrations (0.25 wt% cipro and 50 % ν/ν phage stock), the resulting phage encapsulation efficiency (EE) reached 29 ± 3 %. Following electrospraying, a modest reduction in phage titer was observed, from 5×10^7 to 1.4×10^7 PFU/mg, suggesting good preservation of phage viability during the electrospraying process. The cipro loading reached 0.20 ± 0.01 %, with an EE of 79.9 ±2.2 %. In addition to spherical morphology and efficient phage loading, the particles exhibited a rapid initial release of their therapeutic cargo, achieving 98.8 ±4.0 % of phage release and 93.5 ±7.0 % of cipro release within 10 min. The combination of half the minimum heat inhibition concentration (MHIC) of cipro (0.3 μ g/ml) and 10^8 PFU/ml phages completely inhibited the growth of *Pseudomonas aeruginosa* (*P. aeruginosa*) over 30 h, and a co-loaded particle concentration of 333 μ g/ml extended bacterial inhibition for over 40 h. The results provide meaningful guidance for the design and optimization of antibiotic- and phage-loaded microparticles as potential antibacterial formulations for the treatment of bacterial infections.

1. Introduction

Antibiotic resistance remains a major global healthcare challenge, particularly in infections of the oral cavity and outer ear, which are frequently associated with respiratory diseases [1,2]. The rise of multidrug-resistant pathogens has compromised the efficacy of conventional antibiotics, underscoring the urgent demand for alternative treatment strategies [3]. Phages, viruses that selectively infect and destroy bacterial cells, have gained increasing attention as potential antimicrobial agents [3]. However, clinical application of phage therapy is challenged by the swift emergence of phage resistance, as bacteria deploy various defense mechanisms such as adsorption inhibition, DNA degradation, and abortive infection pathways [4].

Under these circumstances, combined phage-antibiotic strategies have demonstrated synergistic effects, leading to more effective bacterial clearance and a lower chance of resistance emergence [5–8]. For

example, phage PEV20 used in conjunction with ciprofloxacin (cipro) demonstrated therapeutic promise against drug-resistant P. aeruginosa strains implicated in respiratory tract infections [6]. Phage therapy combined with sub-minimal inhibitory concentrations (sub-MIC) of cipro has also been found to be effective in controlling P. aeruginosa biofilms [7,8]. Spray dried powders containing both phage PEV20 and cipro have exhibited synergistic bactericidal effects against antibiotic-resistant P. aeruginosa isolates from cystic fibrosis patients [9]. Additionally, in a mouse model of acute pulmonary infection with P. aeruginosa, a spray-dried formulation combining phage PEV20 and cipro achieved superior bacterial eradication and alleviated lung inflammation compared to either component alone [10]. Most notably, cipro has been found to stabilize phages effectively through vitrification and/or hydrogen bonding at 4 $^{\circ}\text{C},$ allowing PEV20-cipro powders to remain biologically and physico-chemically stable for 12 months when stored below 20 % relative humidity (RH) at 4 °C, even without a

E-mail address: g.williams@ucl.ac.uk (G.R. Williams).

^{*} Corresponding author.

stabilizing excipient [11].

Electrospraying (ES) has emerged as a promising technique for fabricating phage-loaded microparticles with well-defined morphology, tunable drug release profiles, and improved stability [12–15]. While its application in phage encapsulation has been demonstrated, the potential of electrospraying for the co-formulation of phages and antibiotics remains unexplored. Given the documented synergistic antibacterial effects of phage-antibiotic combinations [16–20] and the advantages of electrospraying as a scalable and reproducible particle engineering approach [21–24], it was hypothesized that electrosprayed phage-antibiotic particles can enhance bactericidal efficacy while preserving phage viability and stability.

In earlier research, phage-loaded lactose particles were fabricated via ES and their antibacterial efficacy was evaluated [24]. Although the phage-loaded particles inhibited bacterial growth above a certain concentration, they were not able to completely kill the bacteria [24]. Therefore, this study aimed to develop ES lactose particles loaded with phages and cipro. Building on the formulation previously developed for phage loading [24], the initial step involved optimizing the cipro loading, followed by assessing phage stability in the cipro formulation solution. After obtaining a stable and suitable formulation solution, efforts focused on optimizing the phage loading. Subsequently, the formulations were thoroughly characterized including morphology, physicochemical attributes, loading efficiency and release profiles of phage/drug, antimicrobial efficacy, as well as overall stability.

2. Materials and methods

2.1. Materials

Lactose monohydrate (LM, C₁₂H₂₂O₁₁·H₂O, MW 360.30 g/mol), glycerol, sodium chloride (NaCl), potassium hydroxide (KOH), and ciprofloxacin were all obtained from Fisher Scientific. Poly(vinyl alcohol) (PVA, molecular weight approximately 30,000 Da) was sourced from Merck. Tryptic Soy Agar (TSA), Tryptic Soy Broth (TSB), and Mueller Hinton Agar (MHA) were acquired from Sigma-Aldrich for bacterial cultivation and antimicrobial testing. Tris hydrochloride (Tris·HCl) was purchased from EMD Millipore for buffer preparation, while magnesium sulfate heptahydrate (MgSO₄·7H₂O) and Triton X-100 were supplied by Thermo Fisher Scientific. Gelatin, used in buffer preparation, and phosphotungstic acid (PTA) for electron microscopy staining were also obtained from Sigma-Aldrich.

Pseudomonas aeruginosa strain NCTC 12903 was provided by TCS Biosciences. A lytic phage (Neko, 10^{12} PFU/ml), specific to this strain, was isolated from a puddle water sample collected in La Spezia, Italy. The SM buffer formulation included 50 mM Tris-HCl, 0.1 M NaCl, 8 mM MgSO₄·7H₂O, and 0.01 % (w/v) gelatin, with the pH adjusted to 7.5. Deionized water was prepared using a Purite purification system (Triple Red Ltd). Copper grids for TEM analysis (300 mesh, formvar/carboncoated, 3.05 mm) were obtained from TAAB Laboratories Equipment

2.2. Bacterial culture

P. aeruginosa NCTC 12903 was cultured using procedures described in previous work [24]. The pellet was initially resuspended in 1 ml of TSB, transferred into 40 ml of fresh medium, and cultured at 37 $^{\circ}$ C for 24 h (first-generation culture). Following vortexing, 1 ml of the first-generation culture was then placed into 40 ml of prewarmed TSB to initiate subculturing. This subculturing step was repeated to ensure culture consistency, with vortexing prior to each transfer. Subsequently, 5 ml of the overnight culture was transferred into 250 ml of prewarmed TSB, followed by incubation at 37 $^{\circ}$ C. Once the optical density, measured at 600 nm using a CO8000 cell density meter (WPA Biowave), reached 0.4–0.7, the culture was used for cryopreservation and CFU quantification.

For enumeration, a 1:10 dilution was prepared by mixing 0.1 ml of culture with 0.9 ml of sterile PBS, followed by serial tenfold dilutions (10^{-2} to 10^{-7}). From each dilution, 50 μ l aliquots were plated on TSA using a sterile L-spreader. After incubation at 37 °C for 24 h, colonies on plates with 2–300 CFU were counted. Viable counts were determined from the 10^{-5} dilution and calculated as approximately 10^8 CFU/ml. (triplicate plating).

The remaining bacterial culture (OD $_{600}=0.4$ –0.7) was centrifuged at 9500 rpm for 10 min at 4 °C. The pellet was washed three times with sterile PBS, each time involving resuspension, vortexing, and centrifugation. Finally, after resuspension in 20 % (ν/ν) glycerol, samples were distributed into 2 ml cryovials and preserved at -80 °C. TSA streak plates were prepared during each step to confirm culture purity and sterility.

2.3. Phage harvesting and quantification

The Neko phage employed in this study is a member of the Caudoviricetes class and has been identified as a Podovirus in previous work [24]. Phages were obtained through plate amplification, elution with SM buffer, centrifugation, and 0.22 µm filtration. Plaque assays were conducted to quantify phages, following previously published protocols [24]. A 100 µl sample of cryopreserved P. aeruginosa was transferred into 5 ml of TSB for culture initiation and cultured overnight (37 °C). The following day, 1 ml of the overnight culture was sampled, and its optical density at 600 nm was monitored using a CO8000 cell density meter (WPA Biowave). Cultures with an OD₆₀₀ between 0.5 and 0.6, corresponding to exponential growth, were selected for phage infection. Phage infection was initiated by mixing 100 µl of bacterial culture with an equal volume of phage stock, followed by a 30-min incubation at 37 °C to allow adsorption. The phage-bacteria mixture was then combined with partially cooled MHA (4 ml, 2 % w/v) and poured onto presolidified MHA plates, followed by overnight incubation at 37 °C. Successful phage replication was indicated by clear lysis zones, in contrast to the uniformly turbid control plates inoculated with P. aeruginosa alone. For phage recovery, 4 ml of SM buffer was added onto each lytic plate and incubated at 4 °C for 1 h. The phage-containing buffer mixed with molten agar was centrifuged at 6500 rpm for 30 min at 4 °C. The supernatant was then passed through a sterile $0.22~\mu m$ filter and stored at 4 °C for later use.

Phage titers were determined via plaque assay. For subsequent analysis, the recovered phage sample was serially diluted ten-fold in SM buffer. For each dilution, $100~\mu l$ was mixed with $100~\mu l$ of exponentially growing P. aeruginosa (OD $_{600}=0.5$ –0.6), incubated at 37 °C for 30 min, and then combined with 4 ml of 2 % w/ν molten MHA. The mixtures were poured onto MHA plates and incubated overnight at 37 °C. Control plates were prepared by omitting the phage suspension. Following incubation, plates containing 2–300 plaques were selected, and plaqueforming units (PFU/ml) were calculated based on triplicate counts. The final phage titer was quantified at $10^{10}~\rm PFU/ml$.

2.4. Evaluation of phage stability in the formulation solution

Based on prior formulation development [24], the blank formulation solution comprised 40 % w/v LM and PVA (9:1 ratio, w/w) in SM buffer containing Triton-X-100 (0.1 % v/v). Cipro was incorporated at a final concentration of 0.25 % w/w (relative to the total mass of solute), as higher levels were found to cause instability and visible precipitation. Following complete dissolution of LM, PVA, and cipro in the buffer system, phage suspension was introduced to the formulation to achieve a mixture with final concentrations of 0.25 wt% cipro, 20 % v/v phage suspension (phage suspension in SM buffer), 40 % w/v of LM and PVA (9:1 w/w), in SM buffer with Triton-X-100 (0.1 % v/v) (F₁). This solution was left at RT for 24 h. Phage viability was examined at 10 min, 1 h, and 24 h using plaque assays. The negative control consisted of P. aeruginosa without phage exposure. All experiments were performed in triplicate to

ensure reproducibility.

2.5. Preparation of electrosprayed solutions

Following confirmation of phage stability within the ciprocontaining system, solutions for electrospraying were prepared accordingly. An initial step involved dissolving PVA, LM, and cipro in the selected solvent system at $130\,^{\circ}$ C. Upon cooling to ambient temperature, phages were incorporated and mixed thoroughly by vortexing for homogeneous distribution. After confirming the suitability of the resulting mixture for electrospraying, formulation optimization efforts focused on enhancing phage loading efficiency. The final formulation (denoted as F₂) comprised final concentrations of 40 % w/v of total solutes, with lactose and PVA in a 9:1 weight ratio, dissolved in SM buffer supplemented with Triton-X-100 (0.1 % v/v). Cipro and phage were incorporated at final concentrations of 0.25 % wt. and 50 % v/v, respectively.

2.6. Preparation of phage and cipro co-loaded ES particles

Electrospraying was performed using a 1 ml BD Plastipak syringe equipped with a 20G needle (internal diameter of 0.337 mm, Nordson EFD). The tip-to-collector distance was maintained at 20 cm, and the solution was delivered at a constant flow rate of 0.01 ml/h using a syringe pump (KDS100, KD Scientific). An applied voltage of 20 kV was maintained throughout the process for both blank and phage–ciprofloxacin formulations, using a high-voltage power supply (HCP 35-35000, FuG Elektronik). The electrospraying was conducted under ambient conditions, with the temperature kept between 20 and 25 $^{\circ}\text{C}$ and relative humidity controlled within the 25–40 % range.

2.7.4. Fourier-transform infrared spectroscopy (FTIR)

A PerkinElmer Spectrum 100 FTIR spectrometer equipped with attenuated total reflectance (ATR) mode was employed for infrared spectral acquisition. Spectral data were recorded from 4000 to 650 ${\rm cm}^{-1}$ at 1 ${\rm cm}^{-1}$ resolution, averaging four scans per sample.

2.7.5. Phage viability after electrospraying

Approximately 3.40 mg of phage-cipro co-loaded microparticles were dispersed in 0.5 ml of prewarmed SM buffer and incubated at 37 °C under continuous shaking overnight [24]. After incubation, the suspension was serially diluted, and phage infectivity was quantified via plaque assay to calculate the plaque-forming units per milliliter (PFU/ml) and then normalized to plaque-forming units per milligram of particles (PFU/mg) based on particle mass. To validate assay specificity, a negative control using *P. aeruginosa* without phage treatment was included. Encapsulation efficiency (EE, %) was calculated based on the ratio of recovered to theoretical phage titer using the equation below:

$$EE (\%) = [measured PFU/mg]/[theoretical PFU/mg] \times 100\%$$
 (1)

Data are expressed as mean \pm standard deviation (SD) from triplicate trials.

2.7.6. Cipro loading

Cipro content (sample from Section 2.7.5) was determined via UV absorbance measurement at 270 nm using a Spectramax M2e plate reader (Molecular Devices). A standard curve prepared in SM buffer (0.5–15 μ g/ml, R² = 0.9999) was used for quantification. The cipro loading and EE were computed as follows:

Cipro content (%) = (mass of cipro in microparticles/mass of microparticles) \times 100

(2)

2.7. Characterization

2.7.1. Transmission electron microscopy (TEM)

TEM was used to characterize the morphology of the phage–cipro coloaded microparticles. To visualize phages, a 5 μ l droplet of phage suspension was placed onto a sheet of parafilm, and a carbon-coated copper grid was laid on top for 10 min to allow particle adsorption. The grid was then blotted with filter paper and stained for 30s using 2 % (w/v) PTA (pH 7, adjusted with 2 M KOH). Excess stain was then removed by blotting, and the grids were left to dry at ambient conditions. For phage–cipro co-loaded particles, the electrosprayed powders were deposited directly onto carbon-coated copper grids for 10 s, and staining with 2 % PTA subsequently performed. Samples were finally imaged on a Philips CM120 BioTWIN instrument.

2.7.2. Scanning electron microscopy (SEM)

Morphological examination via SEM was carried out using a Phenom Pro system (Thermo Fisher Scientific). Prior to SEM observation, samples were sputter-coated with graphite to enhance conductivity. Particle size measurements were obtained by randomly selecting 200 particles per group from different SEM fields and analyzing them using ImageJ (version 1.52a, National Institutes of Health). Particle sizes are expressed as mean \pm SD. Distribution plots were generated using Origin 2022b (OriginLab Corporation).

2.7.3. X-ray diffraction (XRD)

XRD patterns were recorded using a Rigaku Miniflex 600 (Cu K α radiation, $\lambda=1.5418$ Å). The analysis was conducted at 40 kV and 15 mA, with 2 θ values scanned from 3 $^{\circ}$ to 40 $^{\circ}$ at 5 $^{\circ}$ /min.

$$EE (\%) = (measured cipro content/theoretical content) \times 100$$
 (3)

2.7.7. Phage release

Approximately 3.50 mg of phage and cipro co-loaded microparticles were dispersed in 5 ml of prewarmed SM buffer and incubated at 37 °C with gentle shaking (50 rpm) [24]. Over a 24 h period, 10 μ l aliquots of the release medium were withdrawn at predetermined time points (1, 3, 5, 7, 10, 20, 40, 60, 120, 180, 240, 1440 min) and immediately replaced with 10 μ l of pre-warmed SM buffer. The collected samples were serially diluted, and phage viability was evaluated via plaque assay to establish phage concentration (PFU/ml). A negative control contained *P. aeruginosa* without phages. Cumulative phage release (%) was plotted as a function of time (min), with all experiments performed in triplicate to ensure consistency.

2.7.8. Cipro release

The cipro content in the collected medium (from Section 2.7.7) was measured at 270 nm using a Spectramax M2e microplate reader (Molecular Devices). A standard curve (0.5–15 $\mu g/ml,~R^2=0.9999)$ prepared in SM buffer was used for quantification. The cumulative release (%) was calculated with respect to the total cipro initially incorporated into the particles. All measurements were conducted in triplicate, and data are presented as mean \pm SD.

2.7.9. Antibacterial tests

Isothermal microcalorimetry was employed to investigate the in vitro antimicrobial effect of phages, cipro, combination of phage and cipro as well as phage and cipro co-loaded particles against

P. aeruginosa.

2.7.9.1. Antibacterial activity of phages. Phage suspensions were serially diluted tenfold in SM buffer for further antibacterial testing [24]. Each ampoule (3 ml) contained 2 ml of TSB (37 °C), 30 μl of phage suspension, and 0.94 ml of sterile water. To reach a final volume of 3 ml, 30 μl of bacterial suspension (10^6 CFU/ml) was added. The ampoules were sealed, gently vortexed, and transferred into a Thermal Activity Monitor (TAM, TA Instruments). A 30-min equilibration period at 37 °C preceded data acquisition. Heat flow signals were monitored using Digitam software (version 4.1) with the amplifier sensitivity adjusted to 3000 μW.

Controls consisted of *P. aeruginosa* alone or phage suspension (10^8 PFU/ml) without bacterial cells. Each experimental condition was explored in triplicate, and due to high reproducibility, representative thermograms are presented. Results are expressed as heat flow curves (μW vs h). After each run, the ampoules were opened, and the contents were serially diluted to quantify viable *P. aeruginosa* (CFU/ml) and active phage particles (PFU/ml).

2.7.9.2. Efficacy of cipro. The evaluation of the minimum heat inhibition concentration (MHIC) of free cipro against P. aeruginosa NCTC 12903 was conducted in vitro using TAM. A 1000 $\mu g/ml$ cipro stock was obtained by dissolving the drug in 200 ml of 0.5 % (ν/ν) acetic acid. Serial dilutions using sterile water were performed to obtain 100, 10, and 1 $\mu g/ml$ solutions, which were then passed through 0.22 μm filters [25].

Table S1 (Supplementary material) outlines the solutions prepared for *P. aeruginosa* (NCTC 12903). Each glass ampoule (3 ml) was filled with 2 ml of pre-warmed TSB (37 °C), cipro solution, and sterile water. Then, 30 μ l of bacterial suspension was added, adjusting the final volume to 3 ml. Ampoules were sealed, gently vortexed, and transferred into the TAM for thermal equilibration at 37 °C for 30 min. Thermal output was captured using the Digitam 4.1 software at an amplifier sensitivity of 3000 μ W. Calorimetric curves were displayed as heat flow (μ W) as a function of time (h). A placebo control using *P. aeruginosa* alone was included for comparison. Each test condition was conducted three times, and the heat flow curves demonstrated high reproducibility; one representative curve is shown. The final bacterial inoculum was standardized at 10^6 CFU/ml.

2.7.9.3. Combinations of phages and cipro. After investigating the antibacterial effects of phages and cipro individually, their combined effects were further explored. Three phage concentrations— 10^6 , 10^7 , and 10^8 PFU/ml—were tested in combination with 1/4 MHIC ($0.15 \,\mu g/ml$) or $1/2 \, MHIC$ ($0.3 \,\mu g/ml$) of cipro. The combination antibacterial activity was assessed in vitro using isothermal microcalorimetry, with each condition evaluated in a minimum of three independent replicates. The resulting heat flow profiles demonstrated high reproducibility, and a representative curve is presented. The bacterial inoculation size was standardized at $10^6 \, \text{CFU/ml}$. Upon completion of each TAM measurement, the ampoules were opened and the contents were serially diluted to quantify both CFU/ml and PFU/ml.

2.7.9.4. Antibacterial activity of phage and cipro co-loaded particles. The antibacterial effect of phage–cipro co-loaded particles against P. aeruginosa was also assessed in vitro by TAM. Co-loaded particles were first pre-weighed (0.25, 0.5, 0.75, 1, and 2 mg) for evaluation. In each trial, 2 ml of TSB (pre-equilibrated at 37 °C), 30 μ l of bacterial inoculum, and a predetermined amount of the test sample were added to the ampoules. Sterile water was used to adjust the final volume to 3 ml. The prepared ampoules were subsequently sealed and transferred into the TAM instrument for measurement.

The heat output was recorded as heat flow curves (μW vs h). Experimental controls included bacterial cultures without treatment and those containing the blank particles. Triplicate measurements were

performed for all five concentrations of the phage and cipro co-loaded formulation. Due to the high reproducibility of the thermal profiles, one representative curve per condition is shown. The initial bacterial concentration was maintained at 10⁶ CFU/ml. Upon completion of each TAM experiment, ampoules were opened and the contents were serially diluted to quantify viable bacterial cells (CFU/ml) and infectious phages (PFU/ml).

2.7.10. Stability studies

A newly prepared phage stock solution was thoroughly vortexed and aliquoted into three portions, which were stored at RT, 4 $^{\circ}$ C, and - 20 $^{\circ}$ C to evaluate phage stability over a 2-month period [24]. In parallel, phage and cipro loaded particles fabricated using the same phage batch were stored under identical conditions. For the liquid phage samples, lytic activity was assessed at predetermined intervals via plaque assay. At each time point, phage and cipro loaded particles were resuspended in SM buffer (0.5 ml) and incubated at 37 $^{\circ}$ C with gentle agitation overnight. The recovered solutions were serially diluted and analyzed using plaque assays to determine phage viability, expressed as PFU/ml. Triplicate trials were carried out for each condition, followed by calculation of PFU/mg values.

3. Results

3.1. Phage viability in the formulation solution

Supplementary material Fig. S1 illustrates phage stability in the F_1 formulation (20 % v/v phage+0.25 wt% cipro, 40 % w/v of LM/PVA (9:1 w/w), SM buffer+0.1 % (v/v) Triton-X-100). The viability of the phage suspension in F_1 remained consistent at ca. 10^{10} PFU/ml across the 24 h assessment period, indicating that the solvent and raw materials lactose do not affect phage stability. Therefore, formulation F_1 was taken forward for electrospraying.

3.2. Variation of phage loading

Fig. 1a presents a SEM image of $F_1.$ F_1 yields particles with spherical morphology albeit with a range of sizes (1–7 μm). The mean particle size of F_1 is 1.9 ± 1.7 μm . The phage titer decreased from 3.2×10^7 PFU/mg (theoretical PFU/mg) to 1.2×10^6 PFU/mg after electrospraying. The final phage encapsulation efficiency of F_1 was hence 4 ± 1 %. For F_1 , the cipro loading was determined to be 0.19 ± 0.01 %, with an encapsulation efficiency of 74.8 ± 1.1 %. The PFU/mg of F_1 was considered too low for effective antibacterial activity. Hence, the concentration of phage suspension was increased to 50 % ν/ν in further experiments. The resulting formulation (F_2) consisted of 0.25 wt% cipro and 50 % ν/ν phage suspension within a 40 % w/ν solution of lactose/PVA (9:1 w/w) prepared in SM buffer with 0.1 % v/ν Triton X-100.

As shown in Fig. 1b, F₂ produced particles with uniform spherical

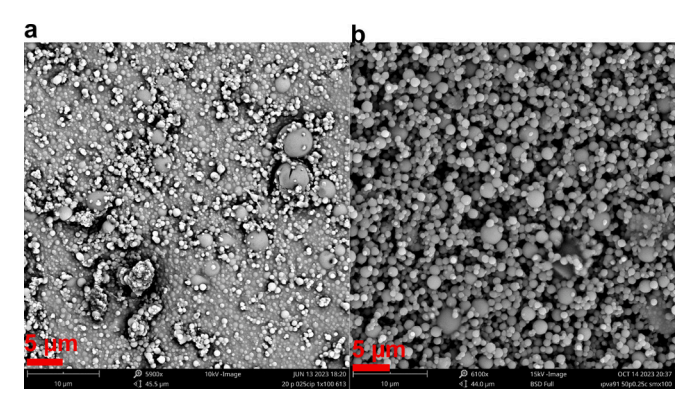


Fig. 1. SEM images of (a) F_1 and (b) F_2 .

morphology. The mean particle size of F_2 is $1.5\pm0.5~\mu m$, with a size range of $1\text{--}3~\mu m$. At 50 % ν/ν phage concentration, phage viability showed greater consistency after the electrospraying process, reducing from 5×10^7 PFU/mg (theoretical PFU/mg) to 1.4×10^7 PFU/mg. The final EE of the phages reached 29 ± 3 %, seven times greater than at 20 % ν/ν phage (F1, 4 ± 1 %). At 50 % ν/ν phage concentration, the higher relative proportion of phages in the mixture may enhance the likelihood of their capture during particle formation, thereby improving the encapsulation efficiency. Therefore, the final concentration of phage was set at 50 % ν/ν . The cipro loading of F_2 was 0.20 \pm 0.01 %, and the EE was 79.9 ± 2.2 %, These values are similar to those of F_1 , despite the higher phage concentration in F_2 .

The properties of F_1 (20 % v/v phage+0.25 wt% cipro) and F_2 (50 % v/v phage+0.25 wt% cipro) were next compared and analyzed. As shown in Table 1, the particle sizes of the formulations appeared similar, indicating that phage loading did not significantly affect particle size, likely due to the relatively small size of phages, which aligns with findings in the literature [26]. Additionally, the low cipro content did not cause notable changes in particle size. However, considering the size distribution (Fig. 2), the F_2 particles with 50 % ν /v phage suspension exhibited a narrower size distribution than F_1 with 20 % ν /v phages. These findings indicate that at elevated phage concentrations, phages may contribute to stabilization by minimizing particle aggregation and promoting a more uniform and concentrated size distribution.

3.3. Characterization

3.3.1. Morphology

The Neko phage employed in this study is a member of the *Caudoviricetes* class and has been identified as a Podovirus. Its morphological and biological characteristics were thoroughly described in earlier work [24]. Fig. 3 displays TEM images of F_1 and F_2 . Phages cannot be observed within F_1 , possibly attributed to the low phage loading. Conversely, nanoscale objects consistent with phages are present within F_2 . This result is in agreement with previous studies [26,27]. Additionally, TEM images reveal a heterogeneous distribution of phages within the F_2 particles. While certain particles exhibit a high local concentration of phage entities, others contain comparatively fewer. This variability might be caused by factors such as differential solvent evaporation rates, variations in particle shrinkage and solidification during electrospraying, as well as potential interactions between phages and co-dissolved solutes [28].

3.3.2. XRD and FTIR

The XRD patterns for the phage and cipro loaded particles are displayed in Fig. S2. The blank formulation and F_2 both exhibit diffuse halos, indicating a lack of crystalline features for both LM and cipro post-electrospraying. This suggests that the materials underwent a crystalline-to-amorphous transformation during processing, consistent with previously reported findings [24,25,29]. FTIR spectra are displayed in Fig. S3. The IR spectra of the blank and F_2 formulations exhibit similar profiles, potentially resulting from the overlap between functional groups on the phages and those present in the excipients, with the latter having a more pronounced influence on the overall spectrum.

3.3.3. Phage release and cipro release

The release of phages from F_2 were monitored over a 24 h period (Fig. 4). Fig. 4 depicts the release profile of F_2 , showing a rapid release of both cipro and phages within the first 10 min. The observed burst release

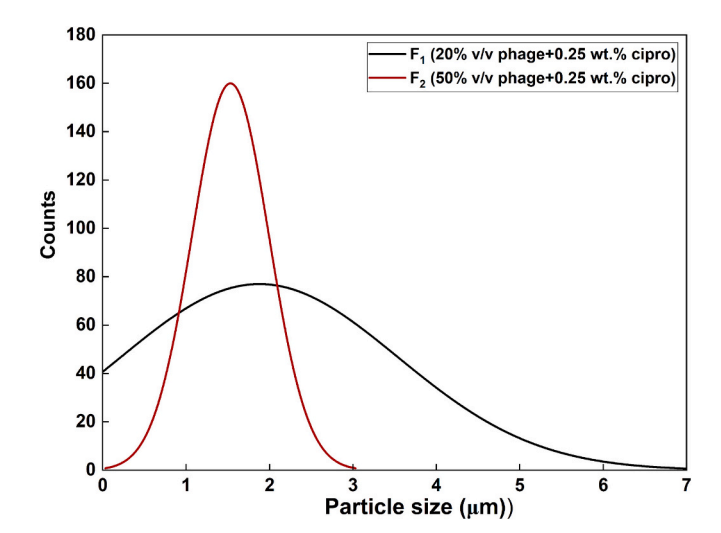


Fig. 2. Size distribution curves of F₁ and F₂.

may result from the fast dissolution of PVA and lactose in the aqueous medium. Additionally, it is observed that both cipro (93.5 \pm 7.0 %) and phage release (98.8 \pm 4.0 %) reach nearly 100 % within 10 min. This rapid release may be suitable in specific scenarios, such as acute bacterial infections or local infection prevention in postoperative or trauma sites [30], where the swift release of drugs and phages can quickly achieve high bactericidal activity. Fig. S4 provides a series of images from plaque assays illustrating that the phage count released remains stable over the 24 h period.

The released phages clearly retain activity over 24 h (see Fig. S4). It should be noted though that rapid drug release may be insufficient for prolonged infections, risking reduced antimicrobial effectiveness [31] and potential bacterial resistance [32]. Given that the release study employed a liquid volume of 5 ml—substantially exceeding the physiological volume typically found at infection sites such as the ear canal, which ranges from approximately 0.6 to 1.8 ml in adults and is even smaller in pediatric patients—this discrepancy should be taken into account when interpreting the release kinetics [33])—the cipro/phage release in practical applications may be slower.

3.3.4. Cipro efficacy

The antimicrobial activity of Neko phages against P. aeruginosa (NCTC 12903) has been discussed in our previous work [24]. Although a clear reduction in bacterial load was observed, complete inhibition could not be achieved even at the highest phage concentration tested (10⁸ PFU/ml) [24]. The MHIC value of cipro against *P. aeruginosa* NCTC 12903 was assessed by isothermal microcalorimetry (Fig. 5). The intricate growth curve observed reflects microbial proliferation within an oxygen-restricted environment, as the enclosed ampoule limits oxygen supply to that initially present in the nutrient medium and the headspace [25,34]. The initial rise in heat flow corresponds to aerobic metabolism during the early exponential growth phase. Around the 5-h mark, a metabolic shift occurs, likely indicating the onset of anaerobic respiration, which is marked by a second rise in metabolic activity [25,34]. As nutrient reserves become exhausted or metabolic byproducts accumulate to inhibitory levels, microbial activity diminishes, ultimately causing the heat output to return to baseline levels [25,34].

Table 1Key formulation parameters for F₁ and F₂.

Formulations	Mean particle size (μm)	Phage titer (10 ⁶ PFU/mg)	Phage EE (%)	Cipro loading (%)	Cipro EE (%)
F ₁ (20 % v/v phage + 0.25 wt% cipro)	1.9 ± 1.7	1.2 ± 0.4	4 ± 1	0.19 ± 0.01	74.8 ± 1.1
F ₂ (50 % v/v phage + 0.25 wt% cipro)	1.5 ± 0.5	14 ± 2	29 ± 3	0.20 ± 0.01	$\textbf{79.9} \pm \textbf{2.2}$

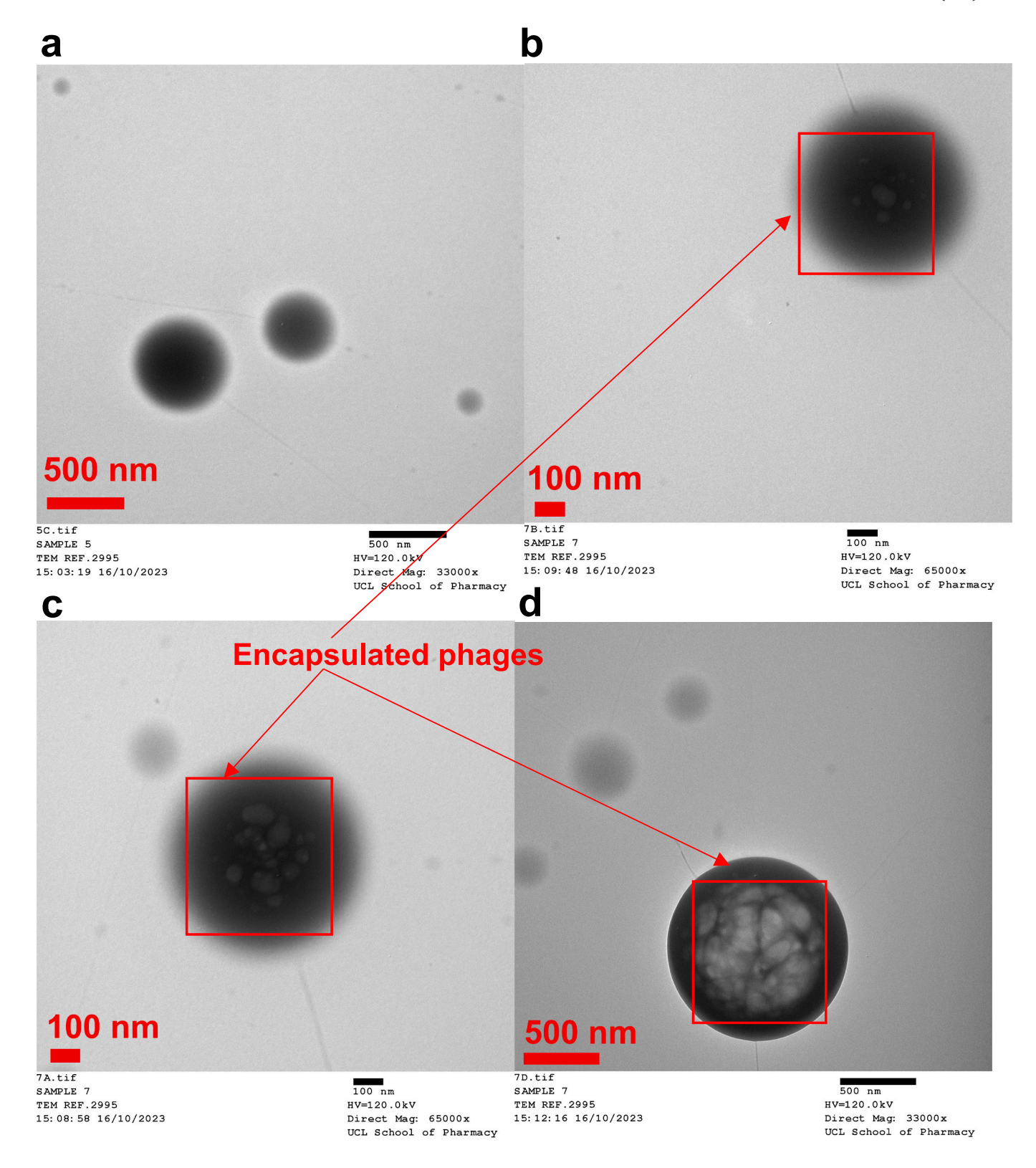


Fig. 3. TEM images of (a) F_1 and (b, c, d) F_2 .

Comparison with the untreated bacterial growth curves (GC) indicates that cipro induces a concentration-dependent delay in the growth of P. aeruginosa. Notably, at concentrations of 0.6 μ g/ml or higher, bacterial proliferation is completely inhibited, as evidenced by the absence of a heat signal. These findings suggest a MHIC of 0.6 μ g/ml,

consistent with the previously reported value for *P. aeruginosa* NCTC 10662 [25,34]. As the heat flow production is quantitatively proportional to the number of viable organisms in the sample [35], the reduction in total heat production indicates a lower number of bacteria in the sample under the influence of cipro.

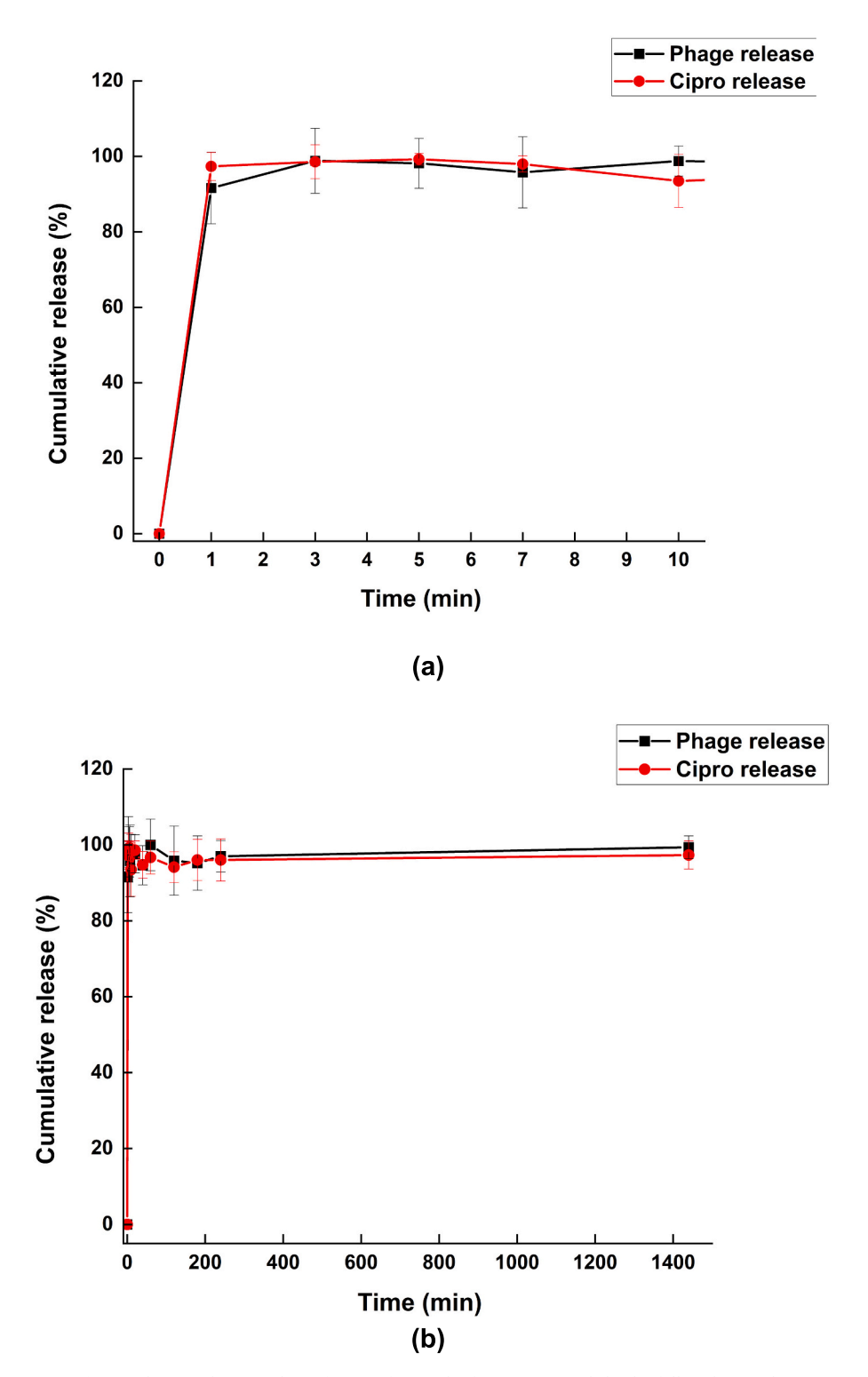


Fig. 4. Phage and cipro release from F_2 for (a) the first 10 min and (b) the full 24 h period.

3.3.5. Combination effects of phages and cipro

3.3.5.1. 1/4 MHIC of cipro +phage. The combination effect of 1/4 of the cipro MHIC (0.15 μ g/ml) and phages against *P. aeruginosa* was determined by TAM (Fig. 6a and Fig. 6b). Both 0.15 μ g/ml cipro and different concentrations of phages (10⁶, 10⁷, 10⁸ PFU/ml) demonstrate antibacterial effects, as indicated by the reduced bacterial counts relative to the GC (Fig. 6c). Notably, 0.15 μ g/ml cipro exhibits stronger antibacterial activity than all the concentrations of phages alone.

Moreover, the combination of phages and 0.15 µg/ml cipro results in enhanced antibacterial efficacy compared to either treatment alone, as shown by the bacterial count comparisons. However, 0.15 µg/ml cipro $+10^6$ PFU/ml appears to promote faster bacterial growth compared to the effects of either component alone. A possible explanation for this phenomenon is that although the low phage concentration of 10^6 PFU/ml may not be sufficient to exert a significant bactericidal effect, the phage infection can induce a stress response in the bacteria [36]. In their efforts to defend against phage infection, the bacteria may alter their

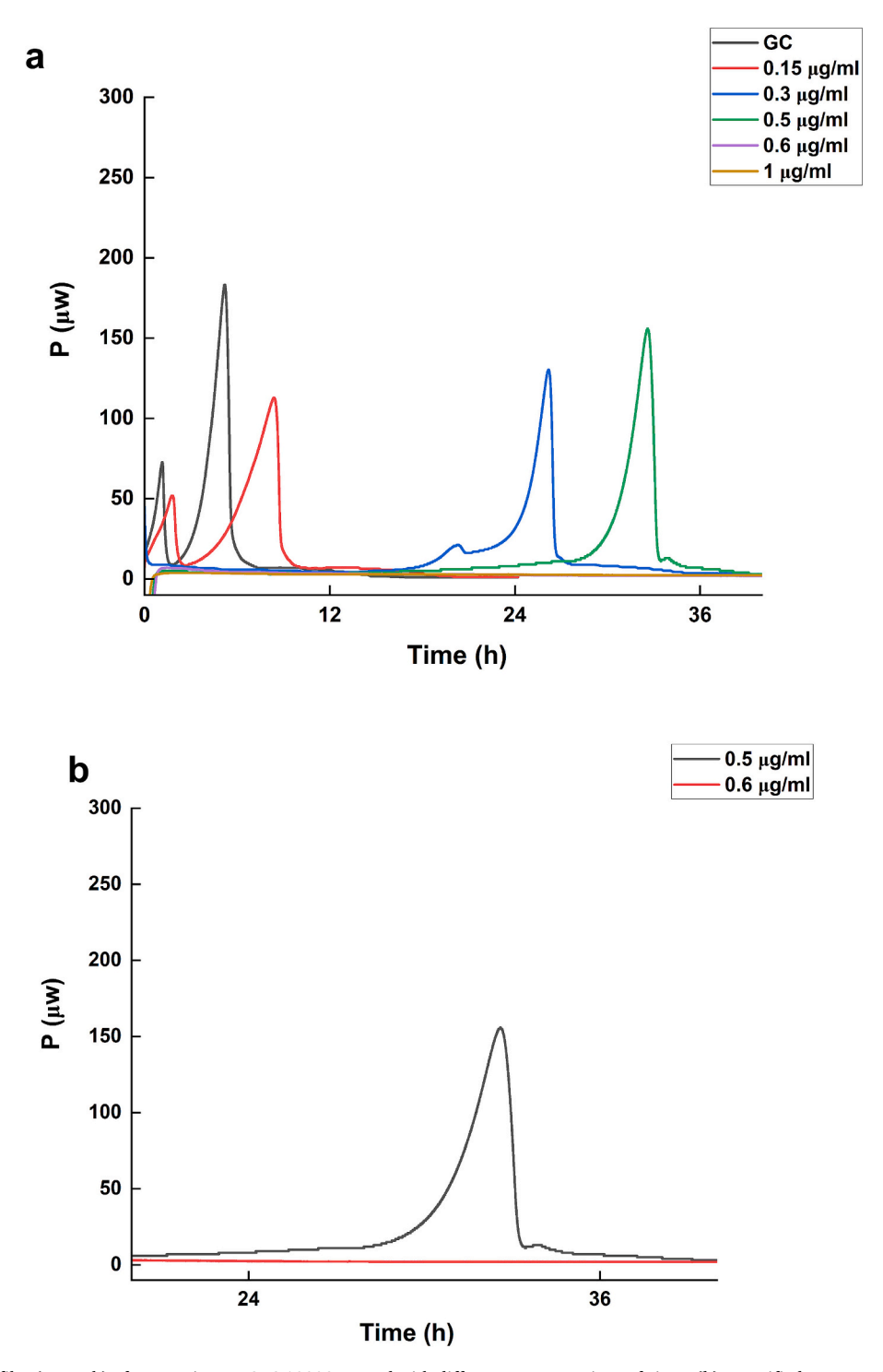


Fig. 5. (a) Heat flow profiles (μ W vs h) of *P. aeruginosa* NCTC 12903 treated with different concentrations of cipro. (b) Magnified segment showing 0.5 and 0.6 μ g/ml cipro treatments within 20–40 h (GC: growth curve). Inoculation density was 10^6 CFU/ml.

gene expression, metabolism, or membrane structure [37]. This adaptive response could inadvertently confer resistance to cipro, ultimately leading to accelerated bacterial growth.

Additionally, it is observed that when bacteria are incubated with the combination of 0.15 µg/ml cipro $+10^8$ PFU/ml, the heat flow curve displays only one peak (Fig. 6a,b), indicative of anaerobic metabolism. In contrast, for 0.15 µg/ml cipro $+10^6$ PFU/ml and 0.15 µg/ml cipro $+10^7$ PFU/ml, the heat flow curves exhibit two peaks, with the first peak representing aerobic metabolism and the second peak indicating anaerobic metabolism. At the lower phage concentrations, bacteria are

less likely to feel the immediate lethal pressure of infection, allowing them to maintain normal aerobic metabolism and efficiently utilize oxygen for energy production. During this phase, the bacteria demonstrate robust growth and metabolic activity, as aerobic metabolism provides greater energy efficiency that supports growth and reproduction [38]. Furthermore, when the aerobic environment becomes unfavorable or oxygen levels decrease, bacteria can easily switch to anaerobic metabolism to adapt to changing conditions [39].

Conversely, at higher phage concentration (0.15 μ g/ml cipro $+10^8$ PFU/ml), phages rapidly infect and lyse the bacteria, presenting an

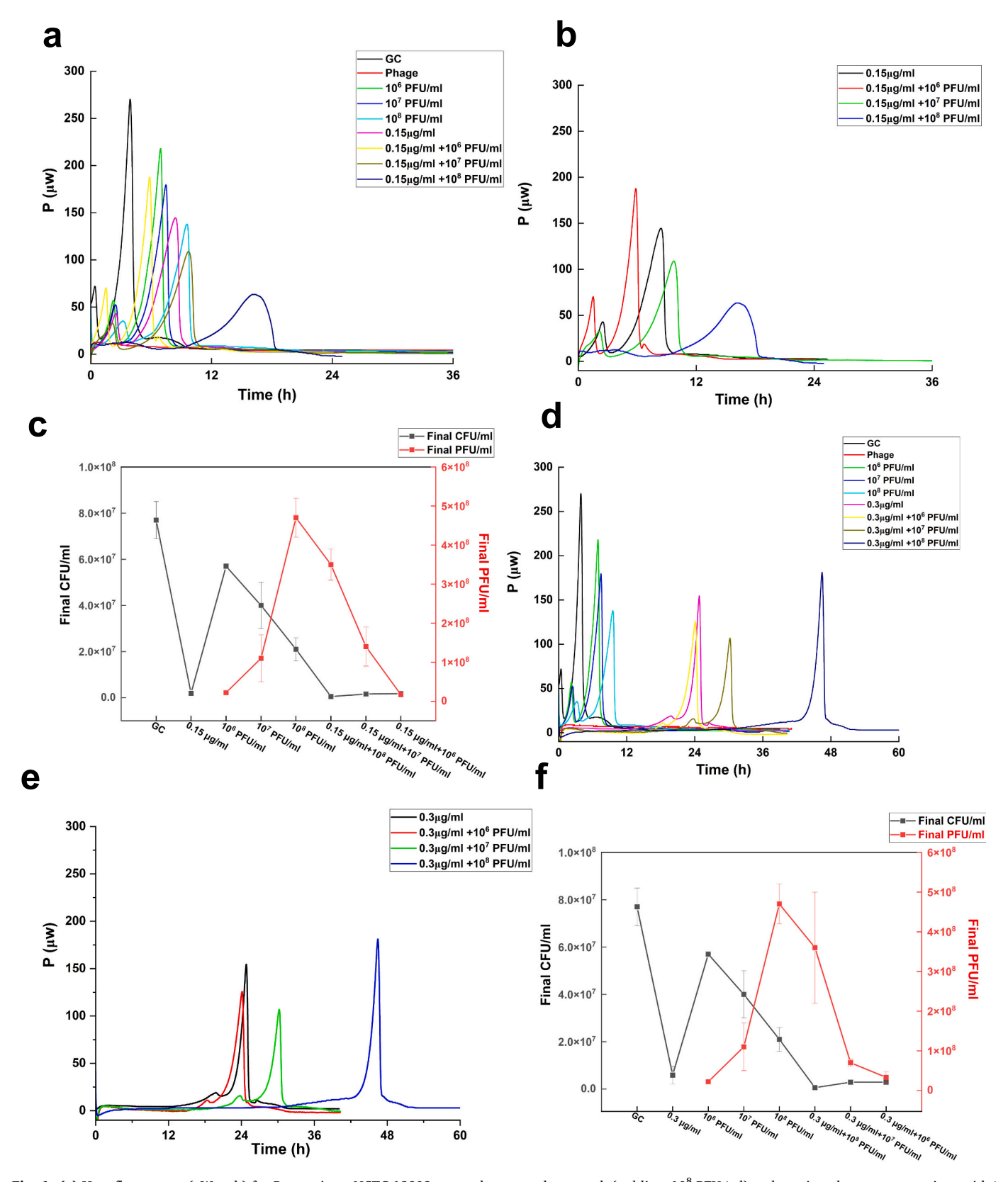


Fig. 6. (a) Heat flow curves (μ W vs h) for *P. aeruginosa* NCTC 12903 exposed to pure phage stock (red line, 10^8 PFU/ml) and varying phage concentrations with/without 0.15 μ g/ml cipro. (b) Comparison of heat flow curves between 0.15 μ g/ml cipro and 0.15 μ g/ml cipro $+10^6$, 10^7 , 10^8 PFU/ml phages. (c) Trends of *P. aeruginosa* CFU/ml value and phage PFU/ml value after exposure to varying phage concentrations with/without 0.15 μ g/ml cipro. (d) Heat flow (μ W) vs time curves for *P. aeruginosa* NCTC 12903 incubated with pure phage (red line, 10^8 PFU/ml, without bacteria) and varying phage concentrations with/without 0.3 μ g/ml cipro. (e) Comparison of heat flow curves between 0.3 μ g/ml cipro and 0.3 μ g/ml cipro + 10^6 , 10^7 , 10^8 PFU/ml phages. (f) Trends of *P. aeruginosa* CFU/ml value and phage PFU/ml value after exposure to varying phage concentrations with/without 0.3 μ g/ml cipro. Initial bacterial inoculum was 10^6 CFU/ml. GC: growth curve.

acute threat of rapid cell death. In this situation, bacteria may prioritize anaerobic metabolism as a survival strategy, enabling them to quickly generate energy and cope with the stress induced by phage infection [40]. This rapid energy acquisition allows bacteria to respond more swiftly, thereby improving their chances of survival [40]. This is consistent with findings in the previous study [41].

Among all the tested combinations, 0.15 µg/ml cipro $+10^8$ PFU/ml phages produces the greatest delay in bacterial growth and the lowest bacterial count, reducing it to $5.1 \pm 0.5 \times 10^5$ CFU/ml (Fig. 6c). Additionally, the final phage count in the 0.15 µg/ml + 10^8 PFU/ml combination was lower than that with 10^8 PFU/ml phages alone, possibly

due to the more effective bactericidal action of this combination, which may have limited phage replication by reducing the available host bacteria. This observation supports the notion that phage proliferation is dependent on the density of bacterial hosts, in agreement with previously documented findings [42].

3.3.5.2.~1/2~MHIC~of~cipro~+~phages. The combination effect of $1/2~MHIC~(0.3~\mu g/ml)$ and phages against P.~aeruginosa was also explored by TAM (Fig. 6d,e). $0.3~\mu g/ml$ cipro leads to a more notable delay in bacterial growth than phages alone at all tested concentrations. Moreover, the combination of phages and $0.3~\mu g/ml$ cipro results in a more

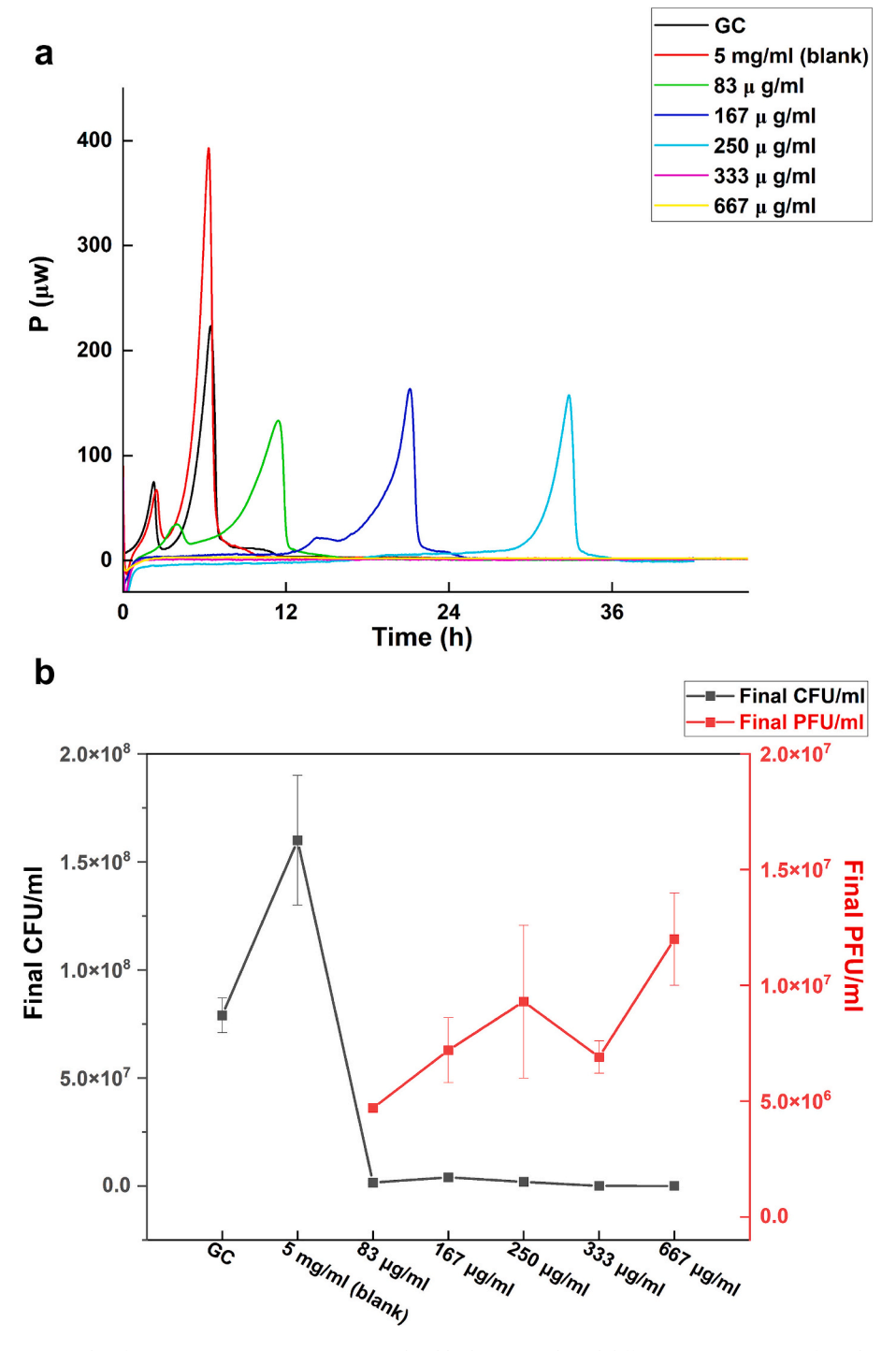


Fig. 7. (a) Heat flow curves (μ W vs h) of *P. aeruginosa* NCTC 12903 exposed to blank (5 mg/ml) and different concentrations of F₂. (b) *P. aeruginosa* CFU/ml value and phage PFU/ml value obtained with varying concentrations of F₂. The bacterial seeding density was 10^6 CFU/ml. GC: growth curve.

pronounced effect than 0.3 µg/ml cipro alone, with the combination of 0.3 µg/ml cipro $+10^7$ PFU/ml delaying the growth of bacteria for up to 18 h, while 0.3 µg/ml cipro $+10^8$ PFU/ml achieves complete bacterial inhibition over 24 h. Additionally, it is observed that the final phage count with 0.3 µg/ml cipro $+10^8$ PFU/ml is lower than that with 10^8 PFU/ml phages alone (Fig. 6f), consistent with the findings observed with 0.15 µg/ml cipro $+10^8$ PFU/ml. Moreover, for 0.3 µg/ml cipro $+10^6$ PFU/ml and 0.3 µg/ml cipro $+10^7$ PFU/ml, the heat flow curves exhibit two peaks (aerobic metabolism and anaerobic metabolism), while the heat flow curve of 0.3 µg/ml cipro $+10^8$ PFU/ml displays only one peak (anaerobic metabolism). This observation is aligned with the findings discussed in Section 3.3.5.1.

3.3.6. Antibacterial effect of cipro + phage loaded particles

P. aeruginosa NCTC 12903 has been shown previously to respond to a blank PVA/LM formulation, with a more pronounced peak implying enhanced bacterial proliferation [24]. The final CFU/ml after incubation with varying blank formulation concentrations (starting at 10⁶ CFU/ml) showed a rise to 10⁸ CFU/ml, suggesting that the blank formulations provide nutrients (mainly lactose) to the bacteria, compared to 10⁷ CFU/ml in the control group [24].

For F_2 (Fig. 7), compared with the GC, bacterial growth is slightly delayed at a particle concentration of 83 µg/ml. As the concentration increases to 167 µg/ml, the start of the peak growth is delayed to 12 h. At 250 µg/ml, growth begins to appear after 20 h. Furthermore, at concentrations of 333 µg/ml or higher, the particles fully suppressed bacterial growth for a duration of 40 h. It can be concluded that the particles maintain a concentration-dependent antibacterial effect of cipro. As the particle concentration increases, the comparison between normalized PFU/ml at the start of incubation and the final PFU/ml after treatment reveals an increase in phage titer, alongside a decrease in bacterial CFU/ml. This suggests that phages actively replicated and lysed bacteria, contributing to the observed antibacterial effect. The rise in phage titer, coupled with the reduction in bacterial count, demonstrates the direct involvement of phages, in synergy with cipro, in driving the antibacterial activity of the formulation.

3.3.7. Cipro and phage-loaded particle stability

Previous work has proved that though phages show stability across all the tested temperatures, -20 °C provided the most favorable environment for preserving phage infectivity and particle count [24]. Fig. 8 illustrates the stability of F_2 at RT, 4, and $-20\,^{\circ}\text{C}$ (all samples came from the same batch), assessed by measuring the PFU/mg at different storage times. The PFU/mg of F2 declines progressively over time under all storage temperatures, with a more pronounced losses observed at RT and 4 $^{\circ}$ C. In contrast, samples stored at -20 $^{\circ}$ C exhibit smaller reductions, suggesting that lower temperatures are more effective in preserving phage viability. The data from week 6 at -20 °C shows a slight increase in phage activity compared to week 4. However, phage activity remained consistently stable at 10⁶ PFU/mg across weeks 1, 2, 4, 6, and 8. The observed fluctuation in week 6 may be attributed to experimental variations, such as minor handling inconsistencies or phage aggregation, which could influence plaque count accuracy. Nevertheless, the overall stability of phage activity across the study period suggests that the formulation remains reasonably stable. These observations are in agreement with previously reported findings [27,43] and align with the results obtained from pure phage suspensions and previously published work [24].

However, akin to the electrosprayed particles containing only phages [24], the co-loaded phage and cipro particles exhibited reduced stability when compared to the phage stock solution (kept at 10¹⁰ PFU/ml across all temperatures over 2 months [24]). Prior research has established a clear hierarchy of excipient efficacy for preserving phage stability in polymer-based systems, ranking SM buffer with sugars as the most effective, followed by SM buffer, sugars, and salts as the least protective [44,45]. In this context, the superior stability of the phage stocks-comprising primarily SM buffer-relative to the solid formulations, which utilize lactose as the protective sugar, aligns with existing findings. Moreover, the absence of humidity control during storage may have further impacted particle stability [24]. This is particularly relevant for storage at lower temperatures (4 $^{\circ}$ C and - 20 $^{\circ}$ C), where transient condensation during handling could have led to partial dissolution of the hygroscopic particles, potentially compromising the integrity of the encapsulated phages.

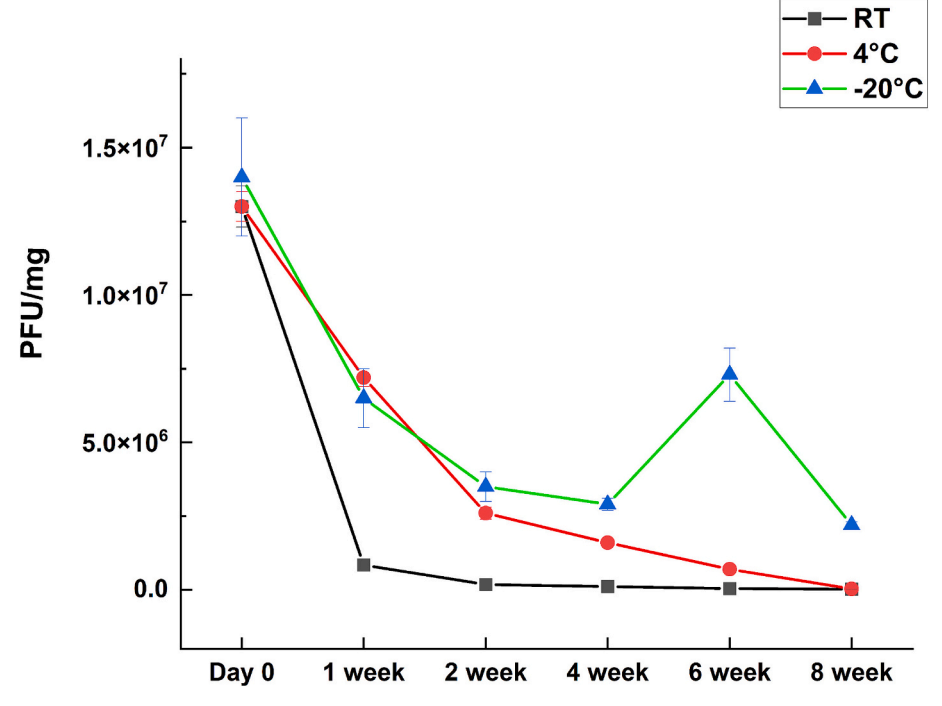


Fig. 8. Stability trends of F_2 at RT, 4, and -20 °C over 8 weeks. The data at -20 °C appear anomalous after 6 weeks, which is attributed to experimental artifacts.

4. Discussion

P. aeruginosa is a prevalent bacterial pathogen responsible for various infections [46]. Combining phages with antibiotics presents a rational and effective strategy to target AMR in this pathogen [4], as bacteria can develop resistance to both treatments [47,48]. However, evolutionary trade-offs make it challenging for bacteria to develop resistance to both antibiotics and phages simultaneously [49]. Previous research has shown that colistin and tobramycin, when combined with phages, exhibit synergistic effects against P. aeruginosa [50,51]. Additionally, studies have reported that amikacin paired with phages also displays synergy against P. aeruginosa biofilms [52] and planktonic cultures [53]. In another study, five FDA-approved antibiotics—cipro, tobramycin, colistin, aztreonam, and amikacin-were tested in combination with phage PEV20 [5]. Among them, amikacin combined with PEV20 showed synergistic effects against two clinical strains, FADD1-PA001 and JIP865, while the cipro-PEV20 combination exhibited the most potent synergistic effect [5]. Moreover, another study confirmed the synergistic antibacterial effect of anti- P. aeruginosa phage PEV31 with cipro [54]. The minimum bactericidal concentration for the combination treatment was 16 µg/ml and 10⁸ PFU/ml, compared to 128 µg/ml required when cipro was used alone. This combination markedly reduced the required cipro dosage to achieve the same bactericidal effect [54]. Due to the lack of standardized methods for evaluating phage-antibiotic interactions, and the incompatibility of the Fractional Inhibitory Concentration (FIC) index (which requires 2-fold dilution scheme) [55], we assessed the interaction based on heat flow inhibition profiles. The observed reduction in the required cipro concentration in the presence of phages indicates an additive effect, consistent with previously reported findings [56].

Phage-antibiotic combination formulations have been developed and proven effective [8,9]. For example, a PEV20-cipro combination dry powder led to a $5.9 \log_{10}$ reduction (p < 0.005) in the bacterial load of P. aeruginosa strains in mouse lungs [9]. Phages are generally considered specific to bacteria and harmless to human cells [57]. The safety of phage PEV20 powder has been evaluated both in vitro and in vivo [58], showing no impact on the viability of human epithelial cells (A549 and HEK239) or macrophages (THP-1) after 24 h of exposure to PEV20. In vivo evaluations also revealed no lung tissue toxicity after phage administration to mice [58].

In this study, we developed a novel electrosprayed particle formulation co-encapsulating the *P. aeruginosa* -specific phage Neko and cipro. To the best of our knowledge, this represents the first use of electrospraying to produce a single dry powder formulation for the combined delivery of a phage and an antibiotic. This strategy offers the potential for combination antibacterial effects and enhanced dosing convenience compared to separate or liquid formulations, particularly in localized therapeutic applications. While it has been reported that the electrospraying process could reduce phage titers by at least one to two orders of magnitude [27], the results of this study showed that the phage titer remained at the same order of magnitude pre- and post-electrospraying. The risk of resistance development with prolonged cipro therapy has been highlighted [59], and bacterial resistance to individual phages is inevitable [60]. The combination of phage and cipro proved highly effective, showing that using only 1/2 MIC of cipro alongside 10⁸ PFU/ ml phage was enough to completely inhibit bacterial growth over 24 h. This aligns with previous research showing synergistic activity of P. aeruginosa-specific phage vB PaeM P6 and sub-MIC cipro (0.75 μg/ ml) in inhibiting biofilm formation and pre-formed biofilms [7].

For treating mild-to-moderate infections, the approved daily oral dose of cipro is 500 mg [61], while the standard intravenous dose is typically 400 mg per day [61]. Additionally, for topical formulations, such as Ciprodex® (0.3 % cipro and 0.1 % dexamethasone suspension), the daily cipro dose for ear infections is at least 0.84 mg (single dose per ear consisting of 0.42 mg cipro and 0.14 mg dexamethasone, twice daily; dosage doubled for bilateral ear infections) [62]. In contrast, this study

demonstrated that only 1 mg of the developed formulation, containing 0.002 mg of cipro, was enough to completely inhibit bacterial growth within 24 h—a lower dose than other formulations.

Although they are potent, the phage and cipro co-loaded particles exhibited suboptimal stability. This is believed to be because lactose served as the primary excipient within the formulation, with PVA included solely to improve the viscosity and electrosprayability of the solution. However, the literature indicates that lactose-only spray dried systems may offer suboptimal protection for phages [63]. This limitation primarily arises from the hygroscopicity and thermodynamic instability of amorphous lactose, which undergoes recrystallization when exposed to moisture. At $\sim\!37$ % RH, its glass transition temperature (Tg) approaches ambient temperature, increasing the risk of physical transformation during storage or handling [64]. Consequently, unless both manufacturing and storage conditions are strictly controlled below this humidity threshold, rapid recrystallization may occur, potentially reducing phage integrity.

In this work, although storage temperature was regulated, humidity control was not implemented during either the manufacturing or storage phases. This likely played a role in the limited stability of the phages encapsulated within our electrosprayed particles. Moving forward, formulation strategies will be optimized to enhance the stability of phage and cipro loaded powders. Future efforts will investigate the incorporation of additional stabilizing excipients, the application of surface coating techniques, and the implementation of controlled-humidity storage conditions to support improved long-term phage viability and broader formulation applicability.

5. Conclusions

This study details the successful creation of cipro and phage loaded electrosprayed (ES) particles. The optimized formulation, comprising 0.25~% wt. cipro and $50~\%~\nu/\nu$ phage suspension, achieved encapsulation efficiencies of 79.9 \pm 2.2 % for cipro and 29 \pm 3 % for phages, with phage viability maintained within the same order of magnitude postprocessing (from 5 \times 10⁷ to 1.4 \times 10⁷ PFU/mg). SEM and TEM confirmed spherical particle morphology and successful phage encapsulation. Rapid release profiles were observed, with over 90 % of both agents released within 10 min. The formulation exhibited strong antibacterial activity, completely inhibiting bacterial growth for 40 h at 333 μg/ml. However, phage viability declined during storage, particularly at room temperature, possibly attributed to the inherent hygroscopicity of the amorphous lactose. Future research will concentrate on excipient optimization and storage improvements to enhance formulation stability. Our results nevertheless highlight the significant potential of an ES dual-loaded dry powder system for localized treatment of bacterial infections in the ear and oral cavity.

CRediT authorship contribution statement

Sai Liu: Writing – review & editing, Writing – original draft, Visualization, Methodology, Investigation, Formal analysis, Data curation, Conceptualization. Andrew Weston: Writing – review & editing, Methodology, Investigation. Giovanni Satta: Writing – review & editing, Resources, Methodology, Funding acquisition, Conceptualization. Sara Bolognini: Writing – review & editing, Resources, Methodology. Mariagrazia Di Luca: Writing – review & editing, Resources, Project administration, Methodology, Funding acquisition. Simon Gaisford: Writing – review & editing, Supervision, Resources, Methodology. Gareth R. Williams: Writing – review & editing, Supervision, Resources, Data curation, Conceptualization.

Declaration of competing interest

The authors declare the following financial interests/personal relationships which may be considered as potential competing interests: Giovanni Satta reports financial support was provided by Medical Research Council. Mariagrazia Di Luca reports financial support was provided by European Union. Mariagrazia Di Luca reports financial support was provided by Tuscany Health Ecosystem. If there are other authors, they declare that they have no known competing financial interests or personal relationships that could have appeared to influence the work reported in this paper.

Acknowledgements

Dr. Giovanni Satta was supported by a Clinical Academic Research Partnership (CARP) fellowship from the Medical Research Council (MR/T023686) UK. Prof. Mariagrazia Di Luca was supported by European Union - Next Generation EU. PNRR MUR M4 C2 Inv. 1.5 CUP I53C22000780001. THE – Tuscany Health Ecosystem; Spoke 7 - Innovating Translational Medicine- Sub-project 5 - Innovative models for management of infections caused by antibiotic-resistant bacteria (Project code: ECS00000017) and POS_PAN-HUB Traiettoria 4. Hub multidisciplinare e interregionale di ricerca e sperimentazione clinica per il contrasto alle pandemie ed. all'antibiotico resistenza CUP I53C22001300001. The phage image in the graphical abstract was generated with Biorender.com.

Appendix A. Supplementary data

Supplementary data to this article can be found online at https://doi.org/10.1016/j.bioadv.2025.214531.

Data availability

Data will be made available on request.

References

- [1] I.S. Gomes-Filho, J.S. Passos, S. Seixas da Cruz, Respiratory disease and the role of oral bacteria, J. Oral Microbiol. 2 (1) (2010) 5811.
- [2] H.R. Hassooni, S.F. Fadhil, R.M. Hameed, A.H. Alhusseiny, S.A.A. Jadoo, Upper respiratory tract infection and otitis media are clinically and microbiologically associated, J. Ideas Health 1 (1) (2018) 29–33.
- [3] D.P. Pires, A.R. Costa, G. Pinto, L. Meneses, J. Azeredo, Current challenges and future opportunities of phage therapy, FEMS Microbiol. Rev. 44 (6) (2020) 684–700.
 - S.J. Labrie, J.E. Samson, S. Moineau, Bacteriophage resistance mechanisms, Nat. Rev. Microbiol. 8 (5) (2010) 317–327.
- [4] T.L. Tagliaferri, M. Jansen, H.-P. Horz, Fighting pathogenic bacteria on two fronts: phages and antibiotics as combined strategy, Front. Cell. Infect. Microbiol. 9 (2019) 22
- [5] Y. Lin, R.Y.K. Chang, W.J. Britton, S. Morales, E. Kutter, H.-K. Chan, Synergy of nebulized phage PEV20 and ciprofloxacin combination against Pseudomonas aeruginosa, Int. J. Pharm. 551 (1–2) (2018) 158–165.
- [6] K. Henriksen, N. Rørbo, M.L. Rybtke, M.G. Martinet, T. Tolker-Nielsen, N. Høiby, et al., P. aeruginosa flow-cell biofilms are enhanced by repeated phage treatments but can be eradicated by phage-ciprofloxacin combination: monitoring the phage-P. aeruginosa biofilms interactions, Pathog. Dis. 77 (2) (2019) ftz011.
- [7] S.S. Sagar, R. Kumar, S.D. Kaistha, Efficacy of phage and ciprofloxacin co-therapy on the formation and eradication of Pseudomonas aeruginosa biofilms, Arab. J. Sci. Eng. 42 (1) (2017) 95–103.
- [8] Y. Lin, R.Y.K. Chang, W.J. Britton, S. Morales, E. Kutter, J. Li, et al., Inhalable combination powder formulations of phage and ciprofloxacin for P. aeruginosa respiratory infections, Eur. J. Pharm. Biopharm. 142 (2019) 543–552.
- [9] Y. Lin, D. Quan, R.Y.K. Chang, M.Y. Chow, Y. Wang, M. Li, et al., Synergistic activity of phage PEV2O-ciprofloxacin combination powder formulation—a proofof-principle study in a P. aeruginosa lung infection model, Eur. J. Pharm. Biopharm. 158 (2021) 166–171.
- [10] Y. Lin, R.Y.K. Chang, W.J. Britton, S. Morales, E. Kutter, J. Li, et al., Storage stability of phage-ciprofloxacin combination powders against Pseudomonas aeruginosa respiratory infections, Int. J. Pharm. 591 (2020) 119952.
- [11] T. Sanders, A. Milicic, E. Stride, Investigating the effect of encapsulation processing parameters on the viability of therapeutic viruses in electrospraying, Pharmaceutics 12 (4) (2020) 388.
- [12] R.M. Eninger, C.J. Hogan Jr., P. Biswas, A. Adhikari, T. Reponen, S.A. Grinshpun, Electrospray versus nebulization for aerosolization and filter testing with bacteriophage particles, Aerosol Sci. Technol. 43 (4) (2009) 298–304.
- [13] J.H. Jung, J.E. Lee, S.S. Kim, Generation of nonagglomerated airborne bacteriophage particles using an electrospray technique, Anal. Chem. 81 (8) (2009) 2985–2990.

- [14] F. Ergin, Effect of freeze drying, spray drying and electrospraying on the morphological, thermal, and structural properties of powders containing phage Felix O1 and activity of phage Felix O1 during storage, Powder Technol. 404 (2022) 117516.
- [15] M. Zhao, H. Li, D. Gan, M. Wang, H. Deng, Q.E. Yang, Antibacterial effect of phage cocktails and phage-antibiotic synergy against pathogenic Klebsiella pneumoniae, Msystems 9 (9) (2024) e00607-24.
- [16] Y.-J. Choi, S. Kim, M. Shin, J. Kim, Synergistic antimicrobial effects of phage vB_ AbaSi_W9 and antibiotics against Acinetobacter baumannii infection, Antibiotics 13 (7) (2024) 680.
- [17] P. Manohar, M. Madurantakam Royam, B. Loh, B. Bozdogan, R. Nachimuthu, S. Leptihn, Synergistic effects of phage–antibiotic combinations against Citrobacter amalonaticus, ACS Infect. Dis. 8 (1) (2022) 59–65.
- [18] E.M. Ryan, M.Y. Alkawareek, R.F. Donnelly, B.F. Gilmore, Synergistic phageantibiotic combinations for the control of Escherichia coli biofilms in vitro, FEMS Immunol Med Microbiol, 65 (2) (2012) 395–398.
- [19] A. Jo, T. Ding, J. Ahn, Synergistic antimicrobial activity of bacteriophages and antibiotics against Staphylococcus aureus, Food Sci. Biotechnol. 25 (2016) 935–940.
- [20] D.N. Nguyen, C. Clasen, G. Van den Mooter, Pharmaceutical applications of electrospraying, J. Pharm. Sci. 105 (9) (2016) 2601–2620.
- [21] S. Spoljaric, Y. Ju, F. Caruso, Protocols for reproducible, increased-scale synthesis of engineered particles—bridging the "upscaling gap", Chem. Mater. 33 (4) (2021) 1099–1115.
- [22] C.U. Yurteri, R.P. Hartman, J.C. Marijnissen, Producing pharmaceutical particles via electrospraying with an emphasis on nano and nano structured particles-a review, Kona Powder Part. J. 28 (2010) 91–115.
- [23] N. Bock, M.A. Woodruff, D.W. Hutmacher, T.R. Dargaville, Electrospraying, a reproducible method for production of polymeric microspheres for biomedical applications, Polymers 3 (1) (2011) 131–149.
- [24] S. Liu, A. Weston, G. Satta, S. Bolognini, M. Di Luca, S. Gaisford, et al., Anti-Pseudomonas aeruginosa phage-loaded electrosprayed lactose particles, J. Drug Deliv. Sci. Technol. 106851 (2025).
- [25] S. Liu, S. Gaisford, G. Williams, Ciprofloxacin-loaded electrosprayed lactose particles, Int. J. Pharm. 2025 (2025) 125748.
- [26] U. Puapermpoonsiri, J. Spencer, C.F. van der Walle, A freeze-dried formulation of bacteriophage encapsulated in biodegradable microspheres, Eur. J. Pharm. Biopharm. 72 (1) (2009) 26–33.
- [27] R. Korehei, J. Kadla, Incorporation of T 4 bacteriophage in electrospun fibres, J. Appl. Microbiol. 114 (5) (2013) 1425–1434.
- [28] A. Jaworek, A.T. Sobczyk, Electrospraying route to nanotechnology: an overview, J. Electrost. 66 (3-4) (2008) 197–219.
- [29] A. Bohr, J. P. Boetker, T. Rades, J. Rantanen, M. Yang, Application of spray-drying and electrospraying/electospinning for poorly watersoluble drugs: a particle engineering approach, Curr. Pharm. Des. 20 (3) (2014) 325–348.
- [30] S. Dhole, C. Mahakalkar, S. Kshirsagar, A. Bhargava, Antibiotic prophylaxis in surgery: current insights and future directions for surgical site infection prevention, Cureus 15 (10) (2023).
- [31] R. Yang, V. Sabharwal, O.S. Okonkwo, N. Shlykova, R. Tong, L.Y. Lin, et al., Treatment of otitis media by transtympanic delivery of antibiotics, Sci. Transl. Med. 8 (356) (2016) 356ra120.
- [32] R.J. Fair, Y. Tor, Antibiotics and bacterial resistance in the 21st century. Perspectives, Med. Chem. 6 (2014). PMC. S14459.
- [33] P.S. Sundar, C. Chowdhury, S. Kamarthi, Evaluation of human ear anatomy and functionality by axiomatic design, Biomimetics 6 (2) (2021) 31.
- [34] S. Liu, S. Gaisford, G.R. Williams, Ciprofloxacin-loaded spray-dried lactose particles: formulation optimization and antibacterial efficacy, Pharmaceutics 17 (3) (2025) 392.
- [35] J. Said, C.C. Dodoo, M. Walker, D. Parsons, P. Stapleton, A.E. Beezer, et al., An in vitro test of the efficacy of silver-containing wound dressings against Staphylococcus aureus and Pseudomonas aeruginosa in simulated wound fluid, Int. J. Pharm. 462 (1–2) (2014) 123–128.
- [36] J.-L. Bru, B. Rawson, C. Trinh, K. Whiteson, N.M. Høyland-Kroghsbo, A. Siryaporn, PQS produced by the Pseudomonas aeruginosa stress response repels swarms away from bacteriophage and antibiotics, J. Bacteriol. 201 (23) (2019), https://doi.org/ 10.1128/jb.00383-19.
- [37] B. Roucourt, R. Lavigne, The role of interactions between phage and bacterial proteins within the infected cell: a diverse and puzzling interactome, Environ. Microbiol. 11 (11) (2009) 2789–2805.
- [38] H.W. Doelle, Bacterial Metabolism, Academic Press, 2014.
- [39] E. Bueno, S. Mesa, E.J. Bedmar, D.J. Richardson, M.J. Delgado, Bacterial adaptation of respiration from oxic to microoxic and anoxic conditions: redox control, Antioxid. Redox Signal. 16 (8) (2012) 819–852.
- [40] S. Hernández, M.J. Vives, Phages in anaerobic systems, Viruses 12 (10) (2020) 1091.
- [41] L. Guosheng, L. Yi, C. Xiangdong, L. Peng, S. Ping, Q. Songsheng, Study on interaction between T4 phage and Escherichia coli B by microcalorimetric method, J. Virol. Methods 112 (1–2) (2003) 137–143.
- [42] R.J. Payne, V.A. Jansen, Understanding bacteriophage therapy as a density-dependent kinetic process, J. Theor. Biol. 208 (1) (2001) 37–48.
- [43] S.S. Leung, T. Parumasivam, A. Nguyen, T. Gengenbach, E.A. Carter, N.B. Carrigy, et al., Effect of storage temperature on the stability of spray dried bacteriophage powders, Eur. J. Pharm. Biopharm. 127 (2018) 213–222.
- [44] C.K. Koo, K. Senecal, A. Senecal, S.R. Nugen, Dehydration of bacteriophages in electrospun nanofibers: effect of excipients in polymeric solutions, Nanotechnology 27 (48) (2016) 485102.

- [45] M. Dai, A. Senecal, S.R. Nugen, Electrospun water-soluble polymer nanofibers for the dehydration and storage of sensitive reagents, Nanotechnology 25 (22) (2014) 225101
- [46] J.A. Driscoll, S.L. Brody, M.H. Kollef, The epidemiology, pathogenesis and treatment of Pseudomonas aeruginosa infections, Drugs 67 (2007) 351–368.
- [47] A.J. Alanis, Resistance to antibiotics: are we in the post-antibiotic era? Arch. Med. Res. 36 (6) (2005) 697–705.
- [48] A.-M. Örmälä, M. Jalasvuori, Phage therapy: should bacterial resistance to phages be a concern, even in the long run? Bacteriophage 3 (1) (2013) e24219.
- [49] O.I. North, E.D. Brown, Phage-antibiotic combinations: a promising approach to constrain resistance evolution in bacteria, Ann. N. Y. Acad. Sci. 1496 (1) (2021) 23, 34
- [50] W.N. Chaudhry, J. Concepcion-Acevedo, T. Park, S. Andleeb, J.J. Bull, B.R. Levin, Synergy and order effects of antibiotics and phages in killing Pseudomonas aeruginosa biofilms, PLoS One 12 (1) (2017) e0168615.
- [51] K. Danis-Wlodarczyk, D. Vandenheuvel, H.B. Jang, Y. Briers, T. Olszak, M. Arabski, et al., A proposed integrated approach for the preclinical evaluation of phage therapy in Pseudomonas infections, Sci. Rep. 6 (1) (2016) 28115.
- [52] A.A.M. Nouraldin, M.M. Baddour, R.A.H. Harfoush, S.A.M. Essa, Bacteriophageantibiotic synergism to control planktonic and biofilm producing clinical isolates of Pseudomonas aeruginosa, Alexandria J. Med. 52 (2) (2016) 99–105.
- [53] J. Uchiyama, R. Shigehisa, T. Nasukawa, K. Mizukami, I. Takemura-Uchiyama, T. Ujihara, et al., Piperacillin and ceftazidime produce the strongest synergistic phage—antibiotic effect in Pseudomonas aeruginosa, Arch. Virol. 163 (2018) 1041–1048
- [54] Q. Hong, R.Y.K. Chang, O. Assafiri, S. Morales, H.-K. Chan, Optimizing in vitro phage-ciprofloxacin combination formulation for respiratory therapy of multi-drug resistant Pseudomonas aeruginosa infections, Int. J. Pharm. 652 (2024) 123853.

- [55] J. Meletiadis, J.W. Mouton, J.F. Meis, P.E. Verweij, In vitro drug interaction modeling of combinations of azoles with terbinafine against clinical Scedosporium prolificans isolates, Antimicrob. Agents Chemother. 47 (1) (2003) 106–117.
- [56] R.Y.K. Chang, T. Das, J. Manos, E. Kutter, S. Morales, H.-K. Chan, Bacteriophage PEV20 and ciprofloxacin combination treatment enhances removal of Pseudomonas aeruginosa biofilm isolated from cystic fibrosis and wound patients, AAPS J. 21 (3) (2019) 49.
- [57] L. Fernández, A. Duarte, A. Rodríguez, P. García, The relationship between the phageome and human health: are bacteriophages beneficial or harmful microbes? Benefic. Microbes 12 (2) (2021) 107–120.
- [58] R.Y.K. Chang, K. Chen, J. Wang, M. Wallin, W. Britton, S. Morales, et al., Proof-of-principle study in a murine lung infection model of antipseudomonal activity of phage PEV20 in a dry-powder formulation, Antimicrob. Agents Chemother. 62 (2) (2018), https://doi.org/10.1128/aac.01714-17.
- [59] R. Cantón, M.-I. Morosini, Emergence and spread of antibiotic resistance following exposure to antibiotics, FEMS Microbiol. Rev. 35 (5) (2011) 977–991.
- [60] P. Hyman, S.T. Abedon, Bacteriophage host range and bacterial resistance, Adv. Appl. Microbiol. 70 (2010) 217–248.
- [61] T. Thai, B.H. Salisbury, P.M. Zito, Ciprofloxacin. StatPearls [internet], StatPearls Publishing, 2023.
- [62] Z. Spektor, M.C. Jasek, D. Jasheway, D.C. Dahlin, D.J. Kay, R. Mitchell, et al., Pharmacokinetics of CIPRODEX® otic in pediatric and adolescent patients, Int. J. Pediatr. Otorhinolaryngol. 72 (1) (2008) 97–102.
- [63] D. Vandenheuvel, A. Singh, K. Vandersteegen, J. Klumpp, R. Lavigne, G. Van den Mooter, Feasibility of spray drying bacteriophages into respirable powders to combat pulmonary bacterial infections, Eur. J. Pharm. Biopharm. 84 (3) (2013) 578-582
- [64] Y.H. Roos, Importance of glass transition and water activity to spray drying and stability of dairy powders, Lait 82 (4) (2002) 475–484.